An Analysis of Nonlocal Scalar Transport in the Convective Boundary Layer Using the Green's Function

FUJIHIRO HAMBA

Institute of Industrial Science, University of Tokyo, Tokyo, Japan

(Manuscript received 30 May 1994, in final form 25 August 1994)

ABSTRACT

The Green's function for scalar fluctuations is introduced into a large eddy simulation of the convective boundary layer to investigate nonlocal scalar transport. This Green's function is used to derive a nonlocal expression for the scalar flux and to evaluate a coefficient called the turbulent diffusivity function. Such an expression shows that scalar transport is nonlocal in both space and time. It is shown that the scalar flux in the middle of the boundary layer is influenced by the scalar gradient in the whole boundary layer. The top-down and bottom-up diffusion as well as the countergradient transport is explained by the turbulent diffusivity function. Moreover, a nonlocal expression for the pressure scalar correlation term in the second-order model is proposed using the same Green's function. It is shown that the nonlocal property of the pressure term accounts for the difference in the return-to-isotropy timescales between the top-down and bottom-up diffusion.

1. Introduction

Modeling of turbulent transport of a scalar is important in predicting scalar distribution in the atmospheric boundary layer. The value of the scalar flux must be evaluated to solve the mean scalar equation. In first-order models, the scalar flux is modeled in terms of the mean scalar. The K theory is one of the first-order models; the scalar flux is assumed to be proportional to the mean scalar gradient and to be directed down the gradient (e.g., Hanna et al. 1981). Although the K theory has been widely used, it is known to be inadequate in some cases (Corrsin 1974). On the other hand, second-order models treat the time advancement equation for the scalar flux by modeling higher-order terms. The second-order model can overcome some defects of the K theory and is becoming a popular tool for the study of the atmospheric boundary layer (Mellor and Yamada 1982; Moeng and Wyngaard 1989). However, the model is still too complicated to apply to large-scale or mesoscale meteorological problems. Thus, there have been several attempts to modify the K theory and to develop more accurate first-order models.

Wyngaard and Brost (1984) showed that the value of the eddy diffusivity in the K theory depends on whether the turbulent mixing is driven by the entrainment flux or the surface flux. This is called the top-down and bottom-up diffusion. This diffusion cannot be explained by the K theory if the eddy diffusivity is assumed to be determined only by the wind turbulence and to be independent of the scalar field. By superposing the top-down and bottom-up scalars, Wyngaard and Brost (1984) derived a generalized eddy diffusivity that depends on both the entrainment flux and the surface flux. Hamba (1993) modified the K theory by introducing the second derivative of the mean scalar to explain the top-down and bottom-up diffusion.

It is known that upward heat flux is accompanied by positive gradient of the potential temperature in the upper half of the convective boundary layer. This countergradient transport cannot be accounted for by the K theory. Deardorff (1966) proposed a countergradient term in addition to the eddy diffusivity term to explain the countergradient transport. Holtslag and Moeng (1991) examined data of large eddy simulation (LES) to obtain an expression for the countergradient term. Hamba (1993) showed that the second-derivative term in the modified K theory also accounts for the countergradient transport.

The K theory has such defects partly because it is a local model; that is, the scalar flux is expressed in terms of the local values of the eddy diffusivity and the scalar gradient. Nonlocal effect is reflected in the second-order model because the scalar flux at a point is connected with those at other points through the equation. Thus several attempts have been done to develop nonlocal first-order models.

Stull (1984) proposed the transilient turbulence theory that describes nonlocal transport using a matrix of mixing coefficients. Ebert et al. (1989) used tracers in their LES to directly obtain the matrix. Fiedler (1984)

Corresponding author address: Dr. Fujihiro Hamba, Institute of Industrial Science, University of Tokyo, 7-22-1, Roppongi, Minato-ku, Tokyo 106, Japan.
E-mail: hamba@iis.u-tokyo.ac.jp

also proposed a similar integral model. Fiedler and Moeng (1985) used scalar profiles obtained from LES to construct the matrix in the integral model. Pleim and Chang (1992) used a nonlocal model named the asymmetrical convective model to apply to regional or mesoscale atmospheric chemical models. In addition to the nonlocal property these models are different from the K theory in the following respect: the K theory expresses the scalar flux in terms of the scalar gradient whereas these models express the right-hand side of the scalar equation in terms of the scalar itself.

On the other hand, Berkowicz and Prahm (1980) proposed a generalization of the K theory; that is, the scalar flux is expressed by a spatial integral of the scalar gradient. The model has a coefficient called the turbulent diffusivity function that corresponds to the eddy diffusivity in the K theory. Nakayama et al. (1988) applied this model to the calculation of the scalar field in the turbulent boundary layer for engineering problems.

In this work we investigate the latter type of nonlocal expression; that is, a generalization of the K theory. We introduce the Green's function for the fluctuating scalar to derive a spatially and temporally nonlocal expression for the scalar flux. In a steady state the expression becomes a spatially nonlocal one that is the same as the model used by Nakayama et al. (1988). The turbulent diffusivity function is directly obtained from LES using the Green's function.

In section 2, LES model and numerical method are described and results are briefly compared with other simulations and observations. In section 3, the Green's function for the fluctuating scalar is introduced to investigate nonlocal properties of the scalar transport. Profiles of the turbulent diffusivity function are obtained to explain the top-down and bottom-up diffusion as well as the countergradient transport. In section 4, the Green's function is used to derive a nonlocal expression for the pressure scalar correlation term in the second-order model.

2. Large eddy simulation

As a subgrid-scale (SGS) model we adopt the one-equation model used by Moeng (1984). The equation for the grid-scale velocity $\bar{u}_i$, the grid-scale potential temperature $\bar{\theta}$, and the SGS turbulent energy $\bar{E}$ ($\equiv \overline{u_i'^2}/2$) are written as

$$\frac{\partial \bar{u}_i}{\partial t} = -\frac{\partial}{\partial x_j}(\bar{u}_i\bar{u}_j) - \frac{\partial \bar{P}}{\partial x_i} + \frac{\partial}{\partial x_j}\left[K_m\left(\frac{\partial \bar{u}_i}{\partial x_j} + \frac{\partial \bar{u}_j}{\partial x_i}\right)\right] + \frac{g}{\theta_0}\bar{\theta}\delta_{i3}, \quad (1)$$

$$\frac{\partial \bar{u}_i}{\partial x_i} = 0, \quad (2)$$

$$\frac{\partial \bar{\theta}}{\partial t} = -\frac{\partial}{\partial x_i}(\bar{u}_i\bar{\theta}) + \frac{\partial}{\partial x_i}\left(K_h\frac{\partial \bar{\theta}}{\partial x_i}\right), \quad (3)$$

$$\frac{\partial \bar{E}}{\partial t} = -\frac{\partial}{\partial x_i}(\bar{u}_i\bar{E}) + K_m\left(\frac{\partial \bar{u}_i}{\partial x_j} + \frac{\partial \bar{u}_j}{\partial x_i}\right)\frac{\partial \bar{u}_i}{\partial x_j} - \frac{g}{\theta_0}K_h\frac{\partial \bar{\theta}}{\partial x_3} + \frac{\partial}{\partial x_i}\left(2K_m\frac{\partial \bar{E}}{\partial x_i}\right) - \epsilon, \quad (4)$$

where g is the gravity acceleration, θ_0 is the mean temperature, δ_{ij} is the Kronecker delta symbol, and summation convention is used for repeated subscripts. The total pressure $\bar{P}$ is given by

$$\bar{P} = \frac{\bar{p}}{\rho_0} + \frac{\overline{u_i'^2}}{3}, \quad (5)$$

where $\bar{p}$ is the pressure and ρ_0 is the fluid density. Coriolis force is neglected in (1) because it has little effect in the convective boundary layer when mean velocity is zero (Ebert et al. 1989). The SGS eddy viscosity K_m, the SGS eddy diffusivity K_h, and the dissipation rate ϵ are modeled as

$$K_m = 0.10l\bar{E}^{1/2}, \quad (6)$$

$$K_h = \left(1 + 2\frac{l}{\Delta S}\right)K_m, \quad (7)$$

$$\epsilon = \left(0.19 + 0.51\frac{l}{\Delta S}\right)\frac{\bar{E}^{3/2}}{l}, \quad (8)$$

respectively. The filter width ΔS and the length scale l are given by

$$\Delta S = (\Delta x_1 \Delta x_2 \Delta x_3)^{1/3}, \quad (9)$$

$$l = \begin{cases} \Delta S, & \text{if } \dfrac{\partial \bar{\theta}}{\partial x_3} \leq 0, \\ \min\left[\Delta S, 0.76\bar{E}^{1/2}\left(\dfrac{g}{\theta_0}\dfrac{\partial \bar{\theta}}{\partial x_3}\right)^{-1/2}\right], & \text{if } \dfrac{\partial \bar{\theta}}{\partial x_3} > 0, \end{cases} \quad (10)$$

where Δx_i is the grid interval in the ith direction.

Here and hereafter, x ($\equiv x_1$) and y ($\equiv x_2$) denote the horizontal coordinates and z ($\equiv x_3$) denotes the vertical coordinate; corresponding velocity components are given by u ($\equiv u_1$), v ($\equiv u_2$), and w ($\equiv u_3$). The computational domain is rectangular; its horizontal size is 5120 m × 5120 m and its vertical size is 3000 m. The number of grid points is 64 × 64 × 50. Since a uniform grid is used, the grid intervals are given by $\Delta x = \Delta y = 80$ m and $\Delta z = 60$ m.

The boundary and initial conditions are almost the same as those used by Nieuwstadt et al. (1991). The periodic boundary condition is used in the horizontal directions. At the top boundary, free-slip conditions are imposed for the velocity and the SGS energy, whereas the gradient of the potential temperature is set to 0.003

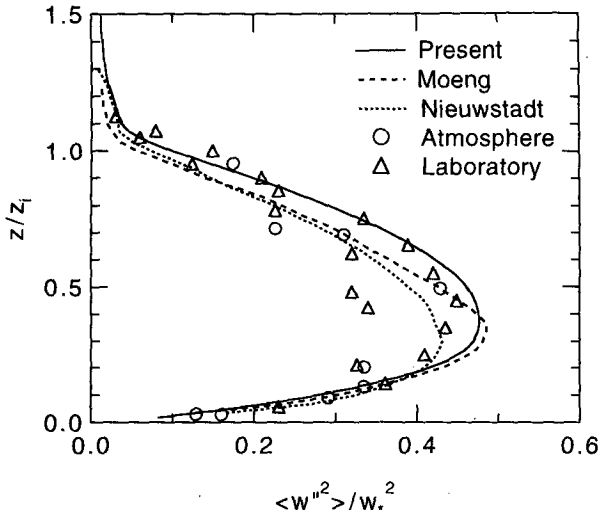

FIG. 1. Profiles of the variance of vertical velocity fluctuation: three curves, results of simulations; two symbols, results of observations.

K m^{-1}. A damping layer is set at the highest nine levels to avoid reflecting gravity waves from the top boundary (Nieuwstadt et al. 1991). At the bottom boundary, a constant heat flux of $Q_S = 0.06$ Km s^{-1} is imposed and the Monin–Obukhov relationship is used to evaluate the momentum flux. The initial condition for the mean potential temperature is given by

$$\langle\theta\rangle = \begin{cases} 300\ (\mathrm{K}), & \text{for } z < 1350\ \mathrm{m}, \\ 300 + 0.003[z\ (\mathrm{m}) - 1350]\ (\mathrm{K}), & \\ & \text{for } z \geq 1350\ \mathrm{m}. \end{cases} \quad (11)$$

The mean velocity is zero; the fluctuating vertical velocity and potential temperature are imposed for $z < 1350$ m using random numbers. Results that will be shown later are normalized in terms of the boundary layer depth z_i and the convective velocity scale w_* defined by

$$w_* = \left(\frac{g}{\theta_0} Q_S z_i\right)^{1/3}. \quad (12)$$

Their initial values are set to $z_{i0} = 1600$ m and $w_{*0} = 1.46$ m s^{-1}. The convective time scale is defined by $t_* = z_{i0}/w_{*0} = 1096$ s.

The equations for the velocity, the potential temperature, and the turbulent energy are calculated by using the second-order finite-difference scheme in space and the Adams–Bashforth scheme in time. The Poisson equation for the pressure is solved by using the Fourier transform in the x and y directions. Time integration is carried out till $t = 12t_*$ with the time step of $\Delta t = 3$ s.

Figure 1 shows the profiles of the variance of vertical velocity fluctuation. A solid line denotes the present result averaged over the horizontal plane and over $9t_* < t < 12t_*$. Dotted lines denote results of two of the simulations by Nieuwstadt et al. (1991). Circle and triangle symbols denote results of atmospheric field tests (Lenschow et al. 1980) and those of laboratory experiments (Willis and Deardorff 1974; Deardorff and Willis 1985), respectively. Although the value obtained from our simulation is somewhat greater than those obtained from the other simulations, the difference is as small as the scatter in the observation data. Figure 2 shows the profiles of the dissipation rate of the turbulent energy. The result of our simulation agrees well with those of the other simulations. The agreement shown in the figures suggests that it is reasonable to use our LES data to investigate the turbulence in the convective boundary layer.

3. Nonlocal expression for scalar flux

In this section we investigate nonlocal properties of the scalar flux to understand the scalar transport in the convective boundary layer. Hereafter, we assume horizontal homogeneity and take an average over the horizontal plane. The equation for the mean scalar is written as

$$\frac{\partial C}{\partial t} = -\frac{\partial}{\partial z}\langle w''c''\rangle, \quad (13)$$

where C and c'' are the mean and fluctuating scalars, respectively, w'' is the vertical component of the fluctuating velocity, $\langle\ \rangle$ denotes the horizontal average, and the molecular diffusivity is neglected. In first-order models the scalar flux $\langle w''c''\rangle$ must be modeled in terms of the mean scalar to close (13). In the K theory, or the eddy-diffusivity model, the scalar flux is assumed to be proportional to the mean scalar gradient as follows:

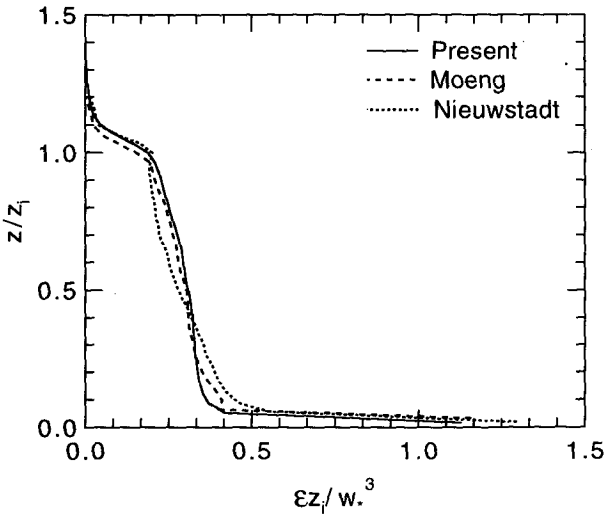

FIG. 2. Profiles of the dissipation rate of the turbulent energy.

$$\langle w''c''\rangle = -K\frac{\partial C}{\partial z}, \tag{14}$$

where K is the eddy diffusivity. This is a local transport model; that is, the flux at height z is evaluated in terms of the scalar gradient at the same height. This approximation is valid only if the turbulence length scale is much shorter than the length scale of the mean scalar field. The turbulence length scale of the convective boundary layer can be roughly estimated by

$$l_T = \frac{k^{3/2}}{\epsilon} \approx 1500 \text{ m}, \tag{15}$$

where k is the turbulent kinetic energy and ϵ is its dissipation rate. This length scale is comparable to the depth of the boundary layer. This means that the approximation of local transport given by (14) is not valid for the scalar transport in the convective boundary layer (Corrsin 1974). In fact, the K theory cannot explain some phenomena such as the countergradient transport.

Some nonlocal models were proposed and applied to the transport in the convective boundary layer (Fiedler and Moeng 1985; Ebert et al. 1989; Pleim and Chang 1992). These models are expressed in a discrete form as

$$\frac{\partial C(z_j)}{\partial t} = \sum_k \mathbf{M}_{jk} C(z_k), \tag{16}$$

where $\mathbf{M}_{jk}$ is a matrix of mixing coefficients between layer j and layer k. Equation (16) implies that the transport at height z_j can be affected by the scalar at different height z_k. Fiedler and Moeng (1985) used scalar profiles obtained from the LES by Moeng and Wyngaard (1984) to construct the matrix $\mathbf{M}_{jk}$. Ebert et al. (1989) used tracers in LES to directly obtain the matrix. Pleim and Chang (1992) introduced an asymmetric form between the upward and downward transport to construct the matrix.

As a generalization of the K theory Berkowicz and Prahm (1980) proposed a nonlocal model for the scalar flux as follows:

$$\langle w''c''\rangle(z) = -\int dz' F(z, z')\frac{\partial C}{\partial z'}, \tag{17}$$

where F is the turbulent diffusivity function. Nakayama et al. (1988) used this model to calculate the scalar field in the turbulent boundary layer for engineering problems. This kind of model was also applied to the Reynolds stress and the turbulent diffusion term for the kinetic energy (Nakayama and Vengadesan 1993).

Equations (16) and (17) are basically the same as shown by Fiedler and Moeng (1985). Substituting (17) into (13) and obtaining a difference equation with respect to space leads to (16); the matrix $\mathbf{M}_{jk}$ can be expressed in terms of F and grid intervals. However, (17) is more straightforward than (16) in the sense that the fluctuating scalar is influenced by the mean scalar gradient rather than by the mean scalar itself. This dependence can be easily seen by considering the equation for the fluctuating scalar given by

$$\frac{\partial c''}{\partial t} = -\frac{\partial}{\partial x_i}(u_i''c'') + \frac{\partial}{\partial z}\langle w''c''\rangle - w''\frac{\partial C}{\partial z}. \tag{18}$$

Therefore, in this work we use (17) to investigate nonlocal transport properties.

Now we derive a nonlocal expression for the scalar flux and use LES data to evaluate coefficients. The equation for the grid-scale scalar $\bar{c}$ is written as

$$\frac{\partial \bar{c}}{\partial t} = -\frac{\partial}{\partial x_i}(\bar{u}_i\bar{c}) + \frac{\partial}{\partial x_i}\left(K_h\frac{\partial \bar{c}}{\partial x_i}\right). \tag{19}$$

This equation is the same as that for $\bar{\theta}$ given by (3), although the scalar $\bar{c}$ is passive; that is, it does not exert influence on the velocity field. The equation for the fluctuating part of $\bar{c}$, or the deviation from the horizontal average, can be written as

$$\frac{\partial \bar{c}''}{\partial t} = -\frac{\partial}{\partial x_i}(\bar{u}_i''\bar{c}'') + \frac{\partial}{\partial z}\langle \bar{w}''\bar{c}''\rangle + \frac{\partial}{\partial x_i}\left(K_h\frac{\partial \bar{c}''}{\partial x_i}\right) - \frac{\partial}{\partial z}\left\langle K_h\frac{\partial \bar{c}''}{\partial z}\right\rangle - \bar{w}''\frac{\partial C}{\partial z}. \tag{20}$$

This is the grid-scale counterpart of (18). We can consider the last term in (20) as a kind of external force that drives the fluctuating scalar field. To examine the dependence of $\bar{c}''$ on $\partial C/\partial z$, we introduce the Green's function $\bar{G}$ that satisfies

$$\frac{\partial \bar{G}}{\partial t} = -\frac{\partial}{\partial x_i}(\bar{u}_i''\bar{G}) + \frac{\partial}{\partial z}\langle \bar{w}''\bar{G}\rangle + \frac{\partial}{\partial x_i}\left(K_h\frac{\partial \bar{G}}{\partial x_i}\right) - \frac{\partial}{\partial z}\left\langle K_h\frac{\partial \bar{G}}{\partial z}\right\rangle + \bar{w}''\delta(z - z')\delta(t - t'). \tag{21}$$

Using the Green's function we can formally solve (20) to obtain

$$\bar{c}''(\mathbf{x}, t) = \bar{c}''(\mathbf{x}, 0) - \int_0^{Lz} dz' \int_0^t dt' \bar{G}(x, z'; t, t')\frac{\partial}{\partial z'}C(z', t'), \tag{22}$$

where L_z is the vertical size of the computational domain. Multiplying (22) by $\bar{w}''$ and taking an average gives

$$\langle \bar{w}''\bar{c}''\rangle(z, t) = -\int_0^{Lz} dz' \int_0^t dt' \times \langle \bar{w}''(\mathbf{x}, t)\bar{G}(\mathbf{x}, z'; t, t')\rangle\frac{\partial}{\partial z'}C(z', t'), \tag{23}$$

where t should be large enough for $\langle \bar{w}''(\mathbf{x}, t)\bar{c}''(\mathbf{x}, 0)\rangle$ to be neglected. This equation can be considered a non-

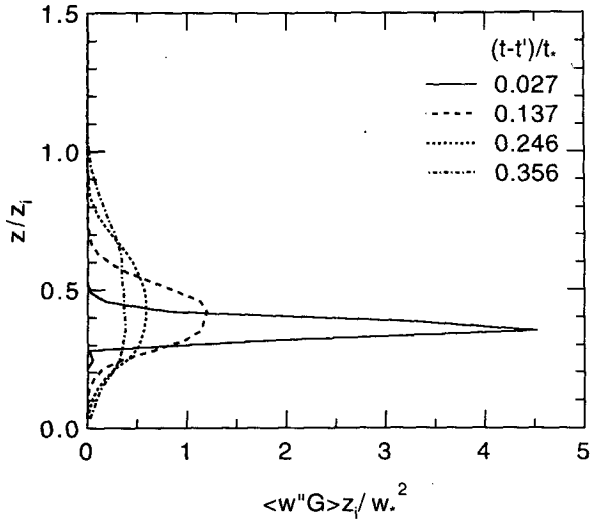

FIG. 3. Profiles of the correlation $\langle \bar{w}''\bar{G}\rangle$ at $z' = 0.351z_i$ and $t' = 9t_*$ as functions of z/z_i.

local expression for the scalar flux. The coefficient $\langle \bar{w}''\bar{G}\rangle$ means the contribution to the scalar flux at (z, t) from the scalar gradient at (z', t'). We should note that the expression is nonlocal not only in space but also in time. In the case of steady turbulence, the scalar gradient does not depend on time. This leads to the following equation:

$$\langle \bar{w}''\bar{c}''\rangle(z) = -\int_0^{Lz} dz' \bar{F}(z, z') \frac{\partial C}{\partial z'}, \qquad (24)$$

where

$$\bar{F}(z, z') = \int_0^t dt' \langle \bar{w}''(\mathbf{x}, t)\bar{G}(\mathbf{x}, z'; t, t')\rangle. \qquad (25)$$

Thus evaluating the Green's function $\bar{G}$ from the LES we can obtain the grid-scale turbulent diffusivity function $\bar{F}$. Equation (24) is the grid-scale counterpart of the nonlocal expression given by (17). Equation (24) is different from (17) in that (24) does not contain the SGS scalar flux $\overline{w'c'}$. Since only the grid-scale scalar is directly calculated in LES, it is difficult to evaluate the nonlocal contribution of $\partial C/\partial z$ to the SGS flux. However, the SGS flux is small compared to the grid-scale flux except for the vicinity of the surface. In addition, the SGS flux can be considered local because in LES it is modeled in terms of local scalar field $\bar{c}$. Thus we will investigate the nonlocal transport of the scalar by considering (24) instead of (17). Detailed procedure of solving the Green's function is given in the appendix.

First, we examine the correlation $\langle \bar{w}''\bar{G}\rangle$ in (23) to investigate both spatially and temporally nonlocal properties of the scalar transport. Figure 3 shows the profiles of $\langle \bar{w}''\bar{G}\rangle(z, z'; t, t')$ at $z' = 0.351z_i$ and $t' = 9t_*$ as functions of z. Four curves correspond to different time intervals $t - t'$. These curves mean how much the scalar gradient at $z' = 0.351z_i$ and $t' = 9t_*$ contributes to the scalar flux at z and t. When $t - t'$ is small, the contribution is almost local; that is, the correlation has its value only around $z = z'$. As $t - t'$ increases, the contribution becomes more nonlocal. We can see that the location of the peak moves upward as $t - t'$ increases. This movement reflects the asymmetry between upward and downward transport. Such asymmetry was also discussed by Ebert et al. (1989). When $t - t' = 0.356t_*$ the peak value decreases to a small value. Since this time interval is smaller than the convective timescale t_*, it seems that the contribution of the scalar gradient to the scalar flux is almost local in time. However, its accumulated contribution is not so local. Figure 4 shows the profiles of the time integral of the correlation given by

$$\int_{t_0}^{t} dt' \langle \bar{w}''(\mathbf{x}, t)\bar{G}(\mathbf{x}, z'; t, t')\rangle, \qquad (26)$$

at $z' = 0.351z_i$ and $t_0 = 9t_*$ as functions of z. We can see some temporally nonlocal contribution when $|z - z'|$ is large. For example, at $z = 0.8z_i$ most of the contribution comes from the period of $t - t_0 > 0.372t_*$. As $t - t_0$ increases, the value of the integral tends to that of the turbulent diffusivity function $\bar{F}$ given by (25).

Next, we examine the turbulent diffusivity function $\bar{F}$. Figure 5 shows the profiles of $\bar{F}(z, z')$ as functions of z'. To obtain good statistical quantities the function is also averaged over $9t_* < t < 12t_*$ (see appendix for details). These curves represent how much the scalar flux at z is affected by the scalar gradient at z'. It is clear that the contribution is nonlocal; the scalar flux is

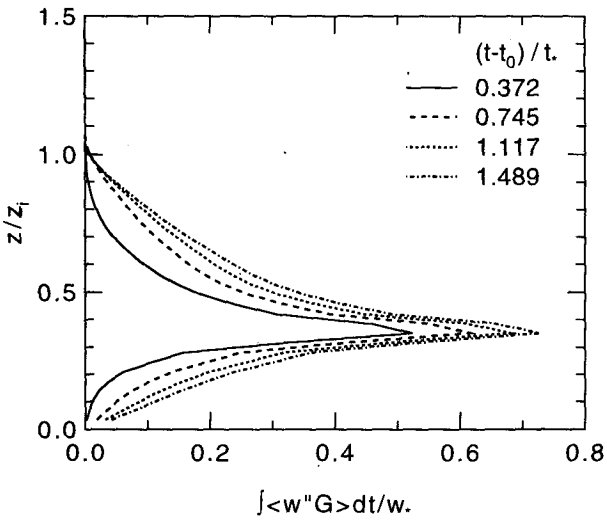

FIG. 4. Profiles of the integral given by (26) at $z' = 0.351z_i$ and $t_0 = 9t_*$ as functions of z/z_i.

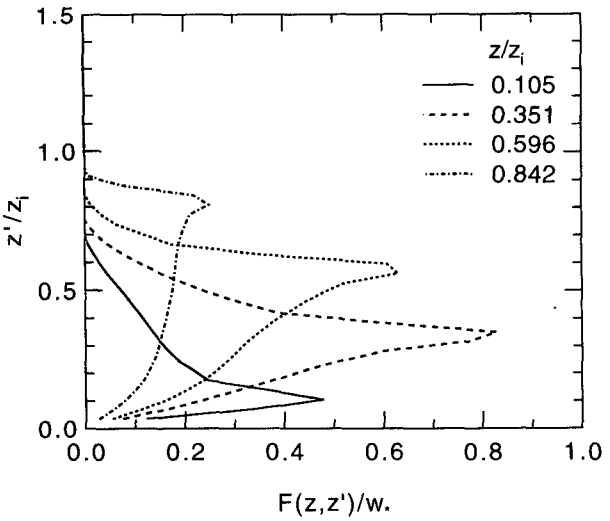

FIG. 5. Profiles of the turbulent diffusivity function as functions of z'/z_i.

influenced not only by local scalar gradient but also by the gradient at different height. In the case of $z = 0.842z_i$, the scalar gradient in the whole boundary layer contributes to the scalar flux. We can also see the asymmetry of the profile; the contribution from the lower layer ($z' < z$) is greater than that from the upper layer ($z' > z$).

To confirm that (24) is a good approximation, we obtain a scalar field by calculating the scalar equation (19) with the boundary conditions $\overline{w'c'} = 1$ at $z = 0$ and $\partial\bar{c}/\partial z = 0$ at $z = L_z$. Figures 6a and 6b show the profiles of the mean scalar and its gradient averaged over the horizontal plane and over $9t_* < t < 12t_*$. The quantities are normalized in terms of z_i and c_* ($\equiv\langle w''c''\rangle/w_*$). The gradient has negative values in the whole boundary layer at $0 < z < z_i$. Figure 7 shows the profiles of the scalar flux. A solid line denotes the flux evaluated by (24), whereas a dashed line denotes the flux directly obtained from the LES. Since the curves do not include the SGS flux, the values near the surface decrease to less than one. The curves are almost linear in height in the middle of the boundary layer. The two curves are in good agreement. This agreement means that the turbulent diffusivity function $\bar{F}$ evaluated using $\bar{w}$ and $\bar{G}$ actually represents the nonlocal contribution to the scalar flux.

The potential temperature is another kind of scalar. Since it satisfies (19), we can examine the heat flux in terms of the same turbulent diffusivity function $\bar{F}$. Figures 8a and 8b show the profiles of the mean potential temperature and its gradient averaged over the horizontal plane and over $9t_* < t < 12t_*$. The gradient is negative in the lower boundary layer because upward heat flux is injected from the surface. The gradient is positive in the upper boundary layer because it is set to a positive value at the top boundary $z = L_z$. Figure 9 shows the profiles of the heat flux. A solid line denotes the flux evaluated by (24), whereas a dashed line denotes the flux directly obtained from the LES. The overall agreement is good although the absolute value of the solid line is somewhat greater than that of the dashed line near the top of the boundary layer at $z = z_i$. This difference is partly because the gradient is very steep near the top of the boundary layer.

The scalar and heat fluxes show different profiles due to the different top-boundary conditions: $\partial C/\partial z = 0$ and $\partial\Theta/\partial z = 0.003\ \mathrm{Km}^{-1}$. The entrainment ratio is defined by the ratio of the entrainment flux at $z = z_i$ to the surface flux at $z = 0$. The ratio for the scalar flux shown in Fig. 7 is about 0.2, whereas that for the heat flux shown in Fig. 9 is about −0.2. Although the fluxes show different types of scalar diffusion, they can be

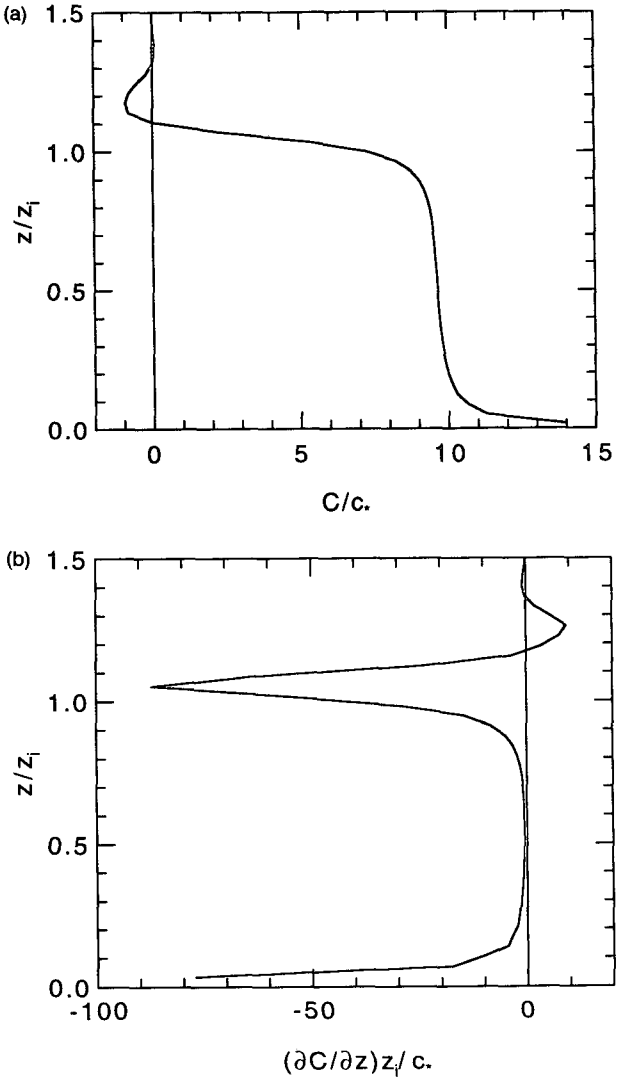

FIG. 6. Profiles of (a) the mean scalar and (b) its gradient.

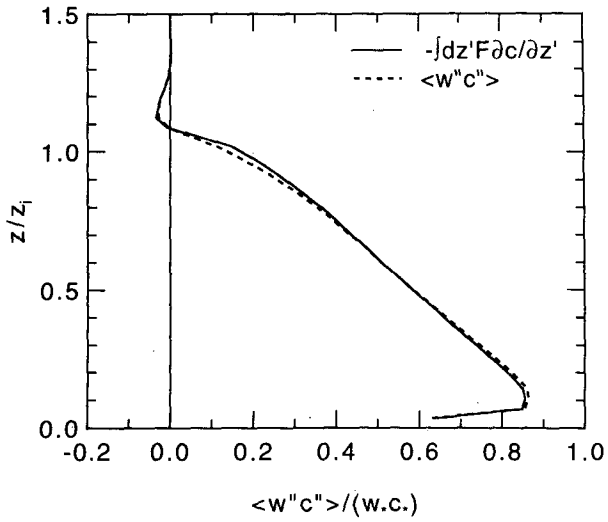

FIG. 7. Profiles of the scalar flux: solid line, evaluated by (24); dashed line, directly obtained from LES.

described in terms of the same turbulent diffusivity function $\bar{F}$. This implies that the nonlocal expression can explain the difference between the top-down and bottom-up diffusion (Wyngaard and Brost 1984). We should note that $\bar{F}$ does not depend on the type of scalar diffusion; it is determined only by the turbulence field. Thus, the difference in the eddy diffusivity between the top-down and bottom-up diffusion is caused by the nonlocal property of the scalar transport. This point was also discussed by Fiedler and Moeng (1985) and by Ebert et al. (1989). It is shown in this work that this nonlocal property can be expressed by a generalization of the K theory.

Hamba (1993) showed that the top-down and bottom-up diffusion can be explained by modifying the K theory as follows:

$$\langle w''c''\rangle = -K\frac{\partial C}{\partial z} + K_2\frac{\partial^2 C}{\partial z^2}. \qquad (27)$$

This modified first-order model describes the difference between the two types of diffusion in terms of the second derivative of the mean scalar. The model can be explained by the Taylor expansion of the nonlocal expression. By expanding $\partial C/\partial z'$ in (17) in powers of $z' - z$ the nonlocal expression can be written as

$$\langle w''c''\rangle(z) = -\int dz' F(z,z')\left[\left.\frac{\partial C}{\partial z'}\right|_{z'=z} + \left.\frac{\partial^2 C}{\partial z'^2}\right|_{z'=z} \times (z'-z) + \frac{1}{2}\left.\frac{\partial^3 C}{\partial z'^3}\right|_{z'=z}(z'-z)^2 + \cdots\right]. \qquad (28)$$

The K theory corresponds to the first term in the Taylor expansion, whereas the modified first-order model corresponds to the first and second terms. The modified first-order model is better than the K theory in the sense that the former reflects more nonlocal property of the diffusion than the latter. To describe the diffusion more accurately it is necessary to use the nonlocal expression.

It is known that the heat flux exhibits the countergradient transport in the convective boundary layer (Deardorff 1966; 1972). In the lower boundary layer the transport is normal; the gradient of the mean potential temperature is negative in Fig. 8, whereas the heat flux is positive in Fig. 9. However, as z increases the values change their sign and the location of the zero point is different between the potential temperature gradient and the heat flux. Both of the two values are positive at $0.418z_i < z < 0.820z_i$. This means the countergradient transport; that is, the heat flux is directed up the gradient of the potential temperature. This transport cannot be explained by the local K theory because negative eddy diffusivity is unphysical.

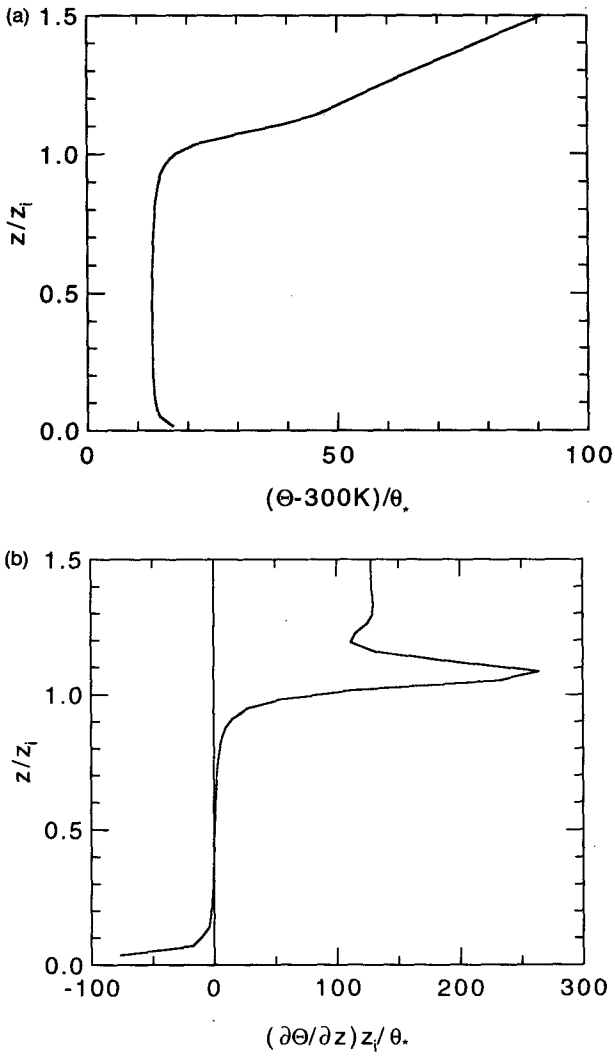

FIG. 8. Profiles of (a) the mean potential temperature and (b) its gradient.

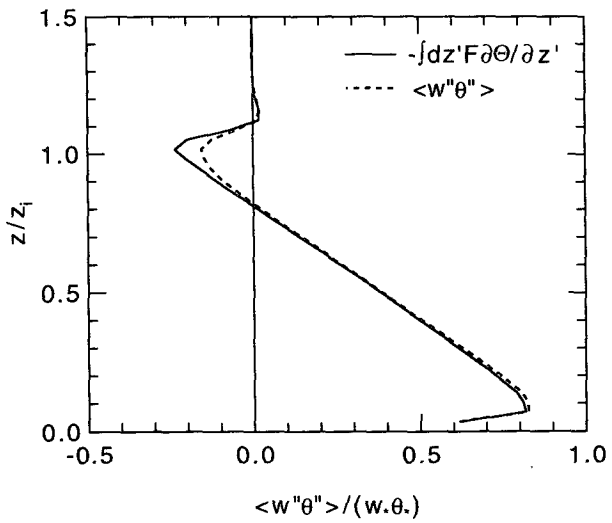

FIG. 9. Profiles of the heat flux: solid line, evaluated by (24); dashed line, directly obtained from LES.

Figure 10 shows the profile of $\bar{F}$ at $z = 0.596z_i$ as a function of z'. This curve implies how much the heat flux at $z = 0.596z_i$ is affected by the gradient of the potential temperature at z'. The curve is divided into two parts in Fig. 10. The gradient of the potential temperature is positive in the upper part and is negative in the lower part. The actual contribution of the two parts can be estimated as

$$\langle \bar{w}''\bar{\theta}'' \rangle (0.596z_i) = -\int_0^{0.418z_i} dz' \bar{F}(0.596z_i, z') \frac{\partial \Theta}{\partial z'} - \int_{0.418z_i}^{z_i} dz' \bar{F}(0.596z_i, z') \frac{\partial \Theta}{\partial z'} = 0.388 - 0.121 = 0.267, \quad (29)$$

where the values are normalized in terms of w_* and θ_*. Although the local contribution from the region around $z' = 0.596z_i$ is negative, the nonlocal contribution from the region of $0 < z < 0.418z_i$ is positive. The absolute value of the latter is greater because the gradient of the potential temperature is much greater as shown in Fig. 8. Therefore, the countergradient transport of the heat flux can be explained by this nonlocal expression; the lower region where the gradient of the potential temperature is negative nonlocally contributes to the middle of the boundary layer to induce positive heat flux.

The difference in the top-down and bottom-up diffusion and that in the countergradient diffusion have also been explained with conventional local models (e.g., Weil 1990; Wyngaard and Weil 1991; Hamba 1993; Holtslag and Moeng 1991). Since local models require less data to parameterize scalar diffusion than our nonlocal expression, local models are more useful in practice. However, the nonlocal expression must be important to better understand the physics of scalar transport and to develop more general turbulence models. Since the size of eddies in the convective boundary layer is as large as the boundary-layer depth, it seems natural and straightforward not to assume the locality. In fact, a simple nonlocal scheme was used to calculate transport of scalars such as chemically reactive species in mesoscale meteorological problems (e.g., Trainer et al. 1987). Our nonlocal expression must be useful to justify and improve such a nonlocal scheme in actual calculations. Moreover, scalar transport caused by turbulence can be found in other geophysical flows as well as in engineering problems. Some specific assumptions in the local models for the convective boundary layer cannot be applied to such flows. For example, the decomposition of top-down and bottom-up scalars assumes that scalar fluxes are linear in height. Such an assumption does not always hold in other turbulent fields. The nonlocal expression is not restricted to linear profiles of fluxes; the nonlocal properties simply lead to the difference in eddy diffusivity between the two scalars. The nonlocal expression must be useful to develop more general turbulence model for scalar transport.

4. Nonlocal expression for pressure scalar correlation

In the second-order model the scalar flux is calculated by integrating the equation

$$\frac{\partial}{\partial t}\langle w''c'' \rangle = -\langle w''^2 \rangle \frac{\partial C}{\partial z} + \frac{g}{\theta_0}\langle \theta''c'' \rangle - \left\langle c'' \frac{\partial p''}{\partial z} \right\rangle - \frac{\partial}{\partial z}\langle w''^2 c'' \rangle. \quad (30)$$

Here and hereafter, p denotes the pressure divided by the

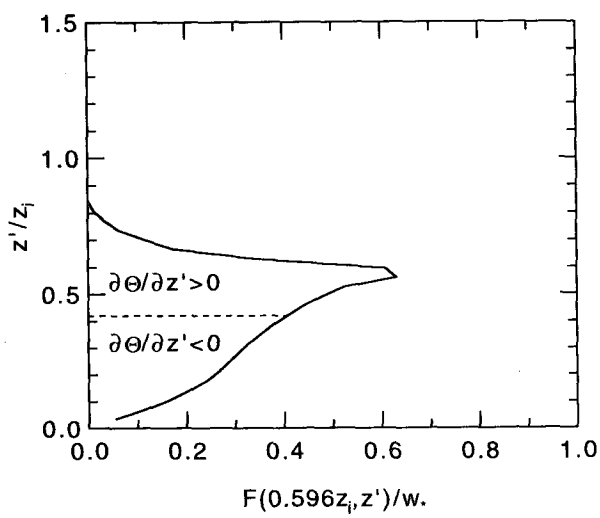

FIG. 10. Profile of the turbulent diffusivity function at $z = 0.596z_i$ as a function of z'/z_i.

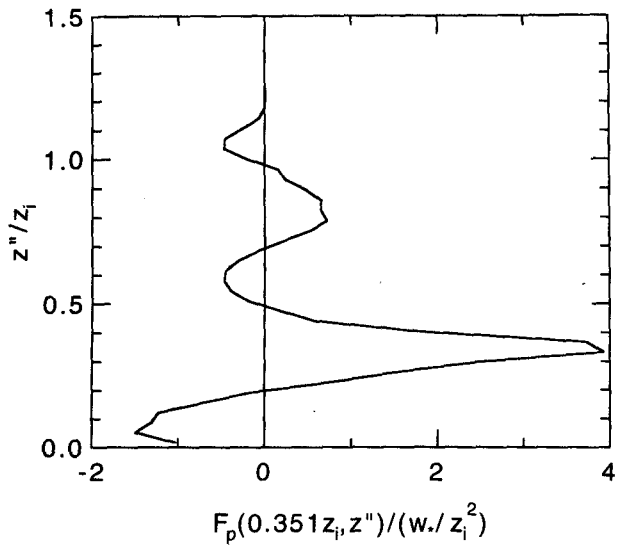

FIG. 11. Profile of the function $\bar{F}_p$ at $z = 0.351z_i$ as a function of z''/z_i.

fluid density. The four terms on the right-hand side are labeled mean-gradient production, buoyant production, pressure scalar correlation, and turbulent diffusion, respectively. To solve the above equation, it is necessary to model the pressure scalar correlation term, which will be referred to as the pressure term, and the turbulent diffusion term. The pressure term can be modeled as

$$\left\langle c'' \frac{\partial p''}{\partial z} \right\rangle = \frac{\langle w''c'' \rangle}{\tau} + A \frac{g}{\theta_0} \langle \theta'' c'' \rangle, \quad (31)$$

where A is a constant that was estimated to be 0.5 by Moeng and Wyngaard (1986). The timescale τ is modeled as a local one-point quantity although the pressure reflects the nonlocal effect of turbulence. In this section we investigate the nonlocal expression for the pressure term in terms of the Green's function $\bar{G}$.

Using (22) and assuming a steady state we can write the pressure term and the temperature scalar correlation term as

$$\left\langle \bar{c}'' \frac{\partial \bar{p}''}{\partial z} \right\rangle (z) = -\int_0^{Lz} dz' \int_0^t dt' \left\langle \bar{G} \frac{\partial \bar{p}''}{\partial z} \right\rangle (z, z'; t, t') \frac{\partial C}{\partial z'}, \quad (32)$$

$$\langle \bar{\theta}'' \bar{c}'' \rangle (z) = -\int_0^{Lz} dz' \int_0^t dt' \langle \bar{\theta}'' \bar{G} \rangle (z, z'; t, t') \frac{\partial C}{\partial z'}, \quad (33)$$

respectively. On the other hand, (24) can be rewritten as

$$\frac{\partial C}{\partial z'} = -\int_0^{Lz} dz \bar{F}^{-1}(z', z) \langle \bar{w}'' \bar{c}'' \rangle (z). \quad (34)$$

where $\bar{F}^{-1}$ satisfies

$$\int_0^{Lz} dz' \bar{F}(z, z') \bar{F}^{-1}(z', z'') = \delta(z - z''). \quad (35)$$

Substituting (34) into (32) and (33) gives

$$\left\langle \bar{c}'' \frac{\partial \bar{p}''}{\partial z} \right\rangle (z) = \int_0^{Lz} dz' \int_0^t dt' \left\langle \bar{G} \frac{\partial \bar{p}''}{\partial z} \right\rangle (z, z'; t, t') \times \int_0^{Lz} dz'' \bar{F}^{-1}(z', z'') \langle \bar{w}'' \bar{c}'' \rangle (z''), \quad (36)$$

$$\langle \theta'' \bar{c}'' \rangle (z) = \int_0^{Lz} dz' \int_0^t dt' \langle \bar{\theta}'' \bar{G} \rangle (z, z'; t, t') \times \int_0^{Lz} dz'' \bar{F}^{-1}(z', z'') \langle \bar{w}'' \bar{c}'' \rangle (z''). \quad (37)$$

Substituting (36) and (37) into (31) yields

$$\left\langle \bar{c}'' \frac{\partial \bar{p}''}{\partial z} \right\rangle - A \frac{g}{\theta_0} \langle \bar{\theta}'' \bar{c}'' \rangle = \int_0^{Lz} dz'' \bar{F}_p(z, z'') \langle \bar{w}'' \bar{c}'' \rangle (z''), \quad (38)$$

where

$$\bar{F}_p(z, z'') = \int_0^{Lz} dz' \int_0^t dt' \left(\left\langle \bar{G} \frac{\partial \bar{p}''}{\partial z} \right\rangle (z, z'; t, t') - A \frac{g}{\theta_0} \langle \bar{\theta}'' \bar{G} \rangle (z, z'; t, t') \right) \bar{F}^{-1}(z', z''). \quad (39)$$

The function $\bar{F}_p$ means a generalization of $1/\tau$ in (31) as a nonlocal quantity. Figure 11 shows the profile of

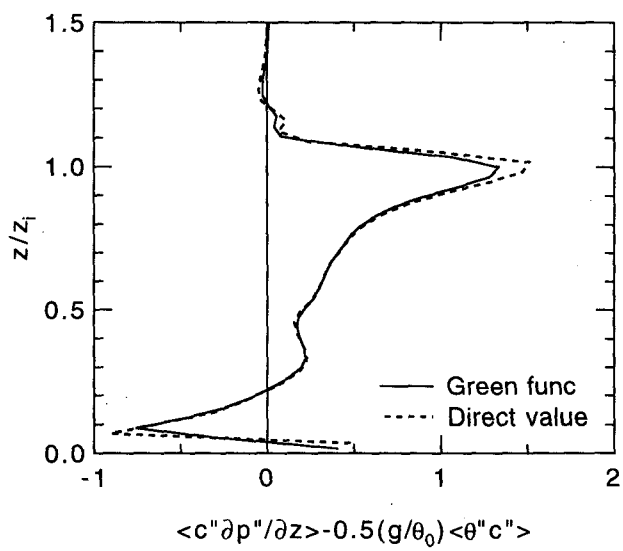

FIG. 12. Profiles of Eq. (38): solid line, right-hand side; dashed line, left-hand side.

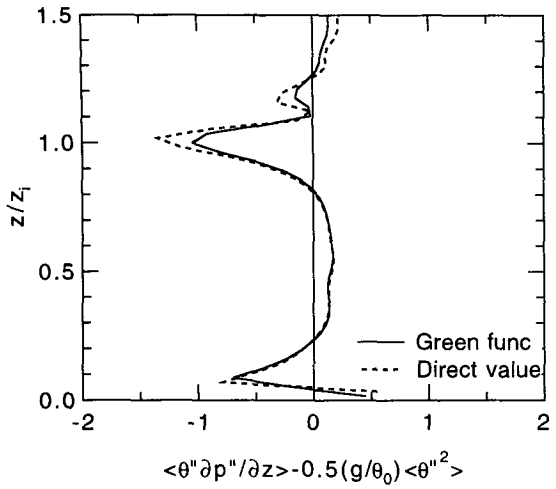

FIG. 13. Profiles of Eq. (40): solid line, right-hand side; dashed line, left-hand side.

$\bar{F}_p(z, z'')$ at $z = 0.351z_i$ as a function of z''. As is the case of $\bar{F}$, the function $\bar{F}_p$ is also averaged over $9t_* < t < 12t_*$ to obtain better statistical quantities. The profile of $\bar{F}_p$ is not so simple as that of $\bar{F}$ shown in Fig. 5. The function $\bar{F}_p$ has both positive and negative values.

Figure 12 shows the profiles of (38) as functions of z. A solid line denotes the value of the right-hand side evaluated using $\bar{F}_p$, whereas a dashed line denotes that of the left-hand side directly obtained from the LES. The two curves are in good agreement. This means that the function $\bar{F}_p$ evaluated using $\bar{G}$ actually satisfies (38).

Since the potential temperature is another kind of scalar, it satisfies the following equation:

$$\left\langle \bar{\theta}'' \frac{\partial \bar{p}''}{\partial z} \right\rangle - A \frac{g}{\theta_0} \langle \bar{\theta}''^2 \rangle = \int_0^{Lz} dz'' \bar{F}_p(z, z'') \langle \bar{w}'' \bar{\theta}'' \rangle (z''). \quad (40)$$

Figure 13 shows the profiles of this equation as functions of z. The two curves agree well. Moeng and Wyngaard (1986) pointed out that the timescale τ should be different between the top-down and bottom-up diffusion. In our nonlocal expression we used the same function $\bar{F}_p$ for the two kinds of fluxes. This implies that the difference in τ between the top-down and bottom-up diffusion stems from the nonlocal property of the scalar transport. This situation is the same as that for the eddy diffusivity.

In Figs. 12 and 13 the values of correlations rapidly change near the surface. The values become negative in some regions and suggest unphysical negative timescales. This behavior may be because the values are the grid-scale part of the correlations and some part remains unresolved. It is necessary to simulate more accurately using more grid points in order to examine the profiles of the correlations in detail.

5. Conclusions

The Green's function for the fluctuating scalar was introduced into a large eddy simulation of the convective boundary layer. The equations for the velocity, the potential temperature, and the SGS energy were integrated in time to obtain a quasi-steady state of turbulence. The equation for the Green's function was also calculated by using the grid-scale velocity and the SGS eddy diffusivity. It was shown that the contribution of the mean scalar gradient to the scalar flux is nonlocal not only in space but also in time. In the case of steady turbulence, the turbulent diffusivity function can be expressed by the time integral of the correlation between the velocity and the Green's function. The profiles of the turbulent diffusivity function show that the scalar flux in the middle of the boundary layer is affected by the scalar gradient in the whole boundary layer.

The scalar and heat fluxes calculated in this work have different entrainment ratios. These two types of diffusion can be expressed by using the same turbulent diffusivity function. This means that the nonlocal expression can account for the top-down and bottom-up diffusion. It was also shown that the countergradient transport of the heat flux can be explained by the nonlocal expression. Positive heat flux in the middle of the boundary layer is shown to be caused nonlocally by negative gradient of the potential temperature in the lower boundary layer.

The pressure scalar correlation term in the second-order model was also examined using the Green's function. A nonlocal expression was proposed for the pressure term. It was shown that the pressure term is affected by the scalar flux at different heights. The difference in the timescale between the top-down and bottom-up diffusion is shown to be explained by the nonlocal expression.

It has been shown that the Green's function for the fluctuating scalar is useful for the analysis of the nonlocal scalar transport. However, since the Green's function evaluated from the LES accounts for only the grid-scale part of the flow, the investigated relationship applies to only the grid-scale parts of quantities. Since the number of the grid points is not so large, the SGS part of some quantities such as the pressure term is not negligible compared to their grid-scale part. Future studies should apply this analysis to more accurate LES using more grid points and to a direct simulation without subgrid models.

Acknowledgments. Part of this work was done while the author was a guest research fellow at Taisei Corporation. This work was partially supported by a Grant-in-Aid from the Ministry of Education, Science, and Culture of Japan.

APPENDIX

Evaluation of the Green's Function and the Turbulent Diffusivity Function

A difference equation for (21) for the Green's function can be obtained in the same manner for the scalar equation. The delta functions $\delta(z - z')$ and $\delta(t - t')$ are replaced by the Kronecker delta symbols $\delta_{K,K'}$ and $\delta_{N,N'}$, where (K, K') and (N, N') are integers denoting z coordinate and time step, respectively. The boundary conditions for $\bar{G}(z, z')$ for each z' are given by $\overline{w'G'} = 0$ at $z = 0$ and $\partial\bar{G}/\partial z = 0$ at $z = L_z$. The conditions are the same as those for the fluctuating scalar.

To obtain the correlation shown in Fig. 3, the difference equation for (21) is integrated in time t for fixed z' and t'. Since (21) includes the SGS eddy diffusivity K_h, the result obtained has model dependence. Direct numerical simulation is more suitable for investigating nonlocal properties. However, such a simulation is not available yet for the convective boundary layer due to its large scale and large Reynolds number.

In a steady state the scalar flux satisfies the following equation:

$$\langle \bar{w}''\bar{c}'' \rangle(z) = -\int_0^{Lz} dz' \bar{F}(z, z') \frac{\partial C}{\partial z'}, \quad \text{(A1)}$$

where $\langle\ \rangle$ denotes the average over the horizontal plane and $C \equiv \langle \bar{c} \rangle$. To make statistical quantities better we also take an average over the period of $9t_* < t < 12t_*$ to obtain the scalar flux and the scalar gradient shown in Figs. 7 and 8, respectively. Corresponding turbulent diffusivity function becomes

$$\frac{1}{3t_*}\int_{9t_*}^{12t_*} dt\bar{F}(z, z') = \frac{1}{3t_*}\int_{9t_*}^{12t_*} dt \int_0^t dt' \langle \bar{w}''(\mathbf{x}, t)\bar{G}(\mathbf{x}, z'; t, t') \rangle. \quad \text{(A2)}$$

This expression includes a double integral with respect to time. It is time consuming to calculate $\bar{G}$ for each t'. Making use of the linearity of the scalar we consider the Green's function defined by

$$\bar{G}_1(\mathbf{x}, z'; t) = \int_0^t dt' \bar{G}(\mathbf{x}, z'; t, t'), \quad \text{(A3)}$$

which satisfies

$$\frac{\partial \bar{G}_1}{\partial t} = -\frac{\partial}{\partial x_i}(\bar{u}_i''\bar{G}_1) + \frac{\partial}{\partial z}\langle \bar{w}''\bar{G}_1 \rangle + \frac{\partial}{\partial x_i}\left(K_h \frac{\partial \bar{G}_1}{\partial x_i}\right) - \frac{\partial}{\partial z}\left\langle K_h \frac{\partial \bar{G}_1}{\partial z} \right\rangle + \bar{w}''\delta(z - z'). \quad \text{(A4)}$$

This Green's function means the response to a temporally constant external force. Instead of (21) we integrate (A4) to obtain $\bar{G}_1$. Then the time-averaged turbulent diffusivity function can be rewritten as

$$\frac{1}{3t_*}\int_{9t_*}^{12t_*} dt\bar{F}(z, z') = \frac{1}{3t_*}\int_{9t_*}^{12t_*} dt\langle \bar{w}''(\mathbf{x}, t)\bar{G}_1(\mathbf{x}, z'; t) \rangle. \quad \text{(A5)}$$

The turbulent diffusivity function $\bar{F}$ shown in Fig. 5 as well as the function $\bar{F}_p$ shown in Fig. 11 are obtained by using the Green's function $\bar{G}_1$.

REFERENCES

Berkowicz, R., and L. P. Prahm, 1980: On the spectral turbulent diffusivity theory for homogenous turbulence. *J. Fluid Mech.*, **100,** 433–448.

Corrsin, S., 1974: Limitations of gradient transport models in random walks and in turbulence. *Advances in Geophysics,* Vol. 18A, Pergamon, 25–60.

Deardorff, J. W., 1966: The counter-gradient heat flux in the lower atmosphere and in the laboratory. *J. Atmos. Sci.*, **23,** 503–506.

——, 1972: Theoretical expression for the countergradient vertical heat flux. *J. Geophys. Res.*, **77,** 5900–5904.

——, and G. E. Willis, 1985: Further results from a laboratory model of the convective planetary boundary layer. *Bound.-Layer Meteor.*, **32,** 205–236.

Ebert, E. E., U. Schumann, and R. B. Stull, 1989: Nonlocal turbulent mixing in the convective boundary layer evaluated from large-eddy simulation. *J. Atmos. Sci.*, **46,** 2178–2207.

Fiedler, B. H., 1984: An integral closure model for the vertical turbulent flux of a scalar in a mixed layer. *J. Atmos. Sci.*, **41,** 674–680.

——, and C.-H. Moeng, 1985: A practical integral closure model for mean vertical transport of a scalar in a convective boundary layer. *J. Atmos. Sci.*, **42,** 359–363.

Hamba, F., 1993: A modified first-order model for scalar diffusion in the convective boundary layer. *J. Atmos. Sci.*, **50,** 2800–2810.

Hanna, S. R., G. A. Briggs, and R. P. Hosker Jr., 1981: *Handbook on Atmospheric Diffusion.* U.S. Department of Energy, 50 pp.

Holtslag, A. A. M., and C.-H. Moeng, 1991: Eddy diffusivity and countergradient transport in the convective atmospheric boundary layer. *J. Atmos. Sci.*, **48,** 1690–1698.

Lenschow, D. H., J. C. Wyngaard, and W. T. Pennel, 1980: Mean-field and second-moment budgets in a baroclinic, convective boundary layer. *J. Atmos. Sci.*, **37,** 1313–1326.

Mellor, G. L., and T. Yamada, 1982: Development of a turbulence closure model for geophysical fluid problems. *Rev. Geophys. Space Phys.*, **20,** 851–875.

Moeng, C.-H., 1984: A large-eddy-simulation model for the study of planetary boundary-layer turbulence. *J. Atmos. Sci.*, **41,** 2052–2062.

——, and J. C. Wyngaard, 1984: Statistics of conservative scalars in the convective boundary layer. *J. Atmos. Sci.*, **41,** 3161–3169.

——, and ——, 1986: An analysis of closures for pressure-scalar covariances in the convective boundary layer. *J. Atmos. Sci.*, **43,** 2499–2513.

——, and ——, 1989: Evaluation of turbulent transport and dissipation closures in second-order modeling. *J. Atmos. Sci.*, **46,** 2311–2330.

Nakayama, A., and S. Vengadesan, 1993: A non-local turbulent transport model. *Proc. Ninth Symp. on Turbulent Shear Flows,* Kyoto, Japan, 26-4-1–26-4-6.

——, H. D. Nguyen, and M. B. Daif, 1988: Nonlocal diffusion model in turbulent boundary layer. *Proc. Third Int. Symp. on Refined*

Flow Modeling and Turbulence Measurements, Tokyo, Japan, Int. Assoc. Hydraulic Res., 305–312.

Nieuwstadt, F. T. M., P. J. Mason, C. H. Moeng, and U. Schumann, 1991: Large-eddy simulation of the convective boundary layer: A comparison of four computer codes. *Proc. Eighth Symp. on Turbulent Shear Flows,* Munich, Germany, 1-4-1–1-4-6.

Pleim, J. E., and J. S. Chang, 1992: A non-local closure model for vertical mixing in the convective boundary layer. *Atmos. Environ.,* **26A,** 965–981.

Stull, R. B., 1984: Transilient turbulence theory. Part I: The concept of eddy mixing across finite distances. *J. Atmos. Sci.,* **41,** 3351–3367.

Trainer, M., E.-Y. Hsie, S. A. McKeen, R. Tallamraju, D. D. Parrish, F. C. Fehsenfeld, and S. C. Liu, 1987: Impact of natural hydrocarbons on hydroxyl and peroxy radicals at a remote site. *J. Geophys. Res.,* **92,** 11 879–11 894.

Weil, J. C., 1990: A diagnosis of the asymmetry in top-down and bottom-up diffusion using a Lagrangian stochastic model. *J. Atmos. Sci.,* **47,** 501–515.

Willis, G. E., and J. W. Deardorff, 1974: A laboratory model of the unstable planetary boundary layer. *J. Atmos. Sci.,* **31,** 1297–1307.

Wyngaard, J. C., and R. A. Brost, 1984: Top-down and bottom-up diffusion of a scalar in the convective boundary layer. *J. Atmos. Sci.,* **41,** 102–112.

——, and J. C. Weil, 1991: Transport asymmetry in skewed turbulence. *Phys. Fluids A,* **3,** 155–162.